

# BAYESIAN HIERARCHICAL MODELS: MODELING THE SPATIOTEMPORAL DISTRIBUTION OF THE RISKS OF PHENOMENA MULTIPLE STRUCTURES

RAKOTONIRINA Alain Barnabé<sup>1</sup>, ANDRIAMANOHSOA Hery-Zo<sup>2</sup>, ROBINSON Matio<sup>3</sup>

<sup>1</sup> PhD student, LRSCA, ED-STII, Antananarivo, Madagascar

<sup>2</sup> Thesis Director, LRSCA, ED-STII, Antananarivo, Madagascar

<sup>3</sup> Thesis co-Director, LRSCA, ED-STII, Antananarivo, Madagascar

## ABSTRACT

A good understanding of the spatiotemporal distribution of complex phenomena and multiple structures (such as the occurrence of fires in the environmental field, epidemic disease in the field of health ...) is an important element for the risk management of these phenomena and the development of strategies. However, the data are subject to complexities caused by heterogeneities among host classes and spatiotemporal processes. This article seeks to suggest or propose a Bayesian spatiotemporal model to modeling and mapping the relative risks of these phenomena in space and time. In this paper, we used spatiotemporal Bayesian hierarchical models to study the relative risk patterns of these phenomena. The R-INLA method with R packages was used for simulations and parameter estimation. The most suitable model is selected using multiple validation criteria (DIC, WAIC, CPO, ...). Among the spatiotemporal models used, the Knorr-Held model with a type III and IV space-time interaction fits well with the data, but type IV seems better than type III. We begin with the introduction to explain the theoretical and problematic context of our work. Then, the spatiotemporal statistical models in the literature review, followed by the proposed methodology which is the Bayesian hierarchical models, followed by an application on the occurrence of fires in the Ankarafantsika National Park (ANP) and ends by conclusion and perspective.

**Keyword:** Phenomena multiple structures, point process, Bayesian Hierarchical models, Spatiotemporal, Integrated Nested Laplace Approximations

## 1. INTRODUCTION

Spatiotemporal statistical modeling is an area that is expanding rapidly and affecting many business sectors as well. All this is due to technological advances in localization systems (AIS, radar, GPS, etc.), Remote sensing (VHF, satellite, GSM, etc.), embedded systems and their low production cost allowed for their deployment. on a large scale.

Many models exist under simplifying assumptions such as stationarity, and separability in space-time models. Indeed, for a long time the spatiotemporal data were treated separately or aggregated (by year, by spatial zone) in order to break down the problem into two modelizations, one in space and the other in time, or to consider matrices of separable covariances. These models are poorly adapted to the complex phenomena observed in practice in the real world.

Consider for example the problem of the environmental domain: the case for the modeling of forest fire occurrences. Indeed, the spatiotemporal distribution of forest fires is very complex in nature with multiple structures (repulsion and aggregation) at different spatial and / or temporal observation scales. The spatiotemporal heterogeneity of fire occurrences will depend on the nature of the terrain (types of vegetation or soil occupation, proximity to urban areas or villages, road network, etc.), the weather, and also the history. because changes in vegetation following fires will affect the probability of occurrence of a fire during the regeneration period.

For this kind of problem, however, statistical methods exist to study the spatiotemporal structure of the data [1][2]. In order to understand and model the stochastic mechanisms of spatiotemporal interaction, it is necessary to place oneself in a non-separable framework. It is in this context of non-separability that spatiotemporal models will be developed during this article.

On the other hand, so far, Markov Chain Monte Carlo (MCMC) techniques have been used for model inference, but these techniques are time-consuming because the spatiotemporal patterns of fire occurrence form a complex class. Advanced MCMC algorithms must be used to obtain reliable posterior estimates and the output of the MCMC may be difficult to interpret for the standard user. Integrated Nested Laplace Approximation (INLA) has recently been proposed as a promising alternative [3]. The methodology offers very precise approximations of marginal laws posteriori in a short calculation time.

In this work, we proposed a point process based on the Bayesian hierarchical model and coupled with the use of INLA (Integrated Nested Laplace Approximation) to avoid computational difficulties. This type of model also makes it possible to take into account certain spatiotemporal variabilities through covariates often collected in practice at different levels of granularity.

## 2. SPATIOTEMPORAL STATISTICAL MODEL

The emergence of work and research in the area of spatiotemporal modeling began about twenty years ago. Indeed, during this period, it turned out that this modeling is a must for all that is the management and manipulation of data that vary in both space and time. While knowing that it is not at all obvious to set up spatiotemporal models, this is due to the complexity of the data involved. As Pekelis [4] has said, pioneering work in this area has been the work of Gail Langran [6] who was the first to see the influence of time in Geographic Information Systems (GIS), Roddick [7], Pekelis [4] which in 2004 made a review of the literature on spatiotemporal models, and more recently of Cressie [8] who wrote a book on statistics for spatiotemporal data. All the work carried out in this field has given rise to several spatiotemporal models of which a family of models has particularly caught our attention, it is the hierarchical Bayesian model.

The structure of spatial data are defined as stochastic process realizations indexed by space

$$Y(s) = \{y(s), s \in \mathcal{D}\} \quad (1)$$

where  $\mathcal{D}$  is a (fixed) subset of dimension  $d$  of the real number  $\mathbb{R}^d$ . In the area-level data structure,  $y(s)$  is a random aggregated value on a surface unit with well-defined boundaries in  $s$ , which defines a countable collection of  $d$ -dimensional spatial units.

The "convolution" model proposed by Besag, York and Mollié in 1991 [9] (better known as the "BYM" model) combines independent unstructured and structured heterogeneity terms in a hierarchical model.

$$\eta_i = b_0 + \vartheta_i + v_i \quad (2)$$

Where  $b_0$  represents the actual parameter corresponding to the global relative risk log-risk in the study area compared to the reference rate, while  $\vartheta_i$  and  $v_i$  respectively correspond to a spatially structured risk effect and a spatially unstructured risk effect for the specific area  $i$ .

On the other hand, spatiotemporal statistical modeling is an important step to understand the mechanisms of certain natural phenomena, such as environmental, geophysical, geological, hydrological and biological phenomena. Indeed, the concentrations of atmospheric pollutants, the meteorological collections, the fields of precipitation, the occurrences of wildfires, etc. are characterized by spatial and temporal variability. So, these phenomena are most often considered as random processes that are generally assumed to be Gaussian. Thus, the measurements of these phenomena in observation sites are seen as realizations of random functions.

The structure of spatiotemporal data is now defined by a process indexed by space and time.

$$Y(s, t) = \{y(s, t), (s, t) \in \mathcal{D} \subset \mathbb{R}^2 \times \mathbb{R}^+\} \quad (3)$$

With  $s$  spotting space and  $t$  time.

As an example, for some model BHM (Bayesian Hierarchical Model), the linear component of the spatiotemporal model for the binary data for a specific response (sample  $i$ , time  $t$ , location  $I$ ) can be defined as follows:

$$\text{logit}(\pi_{itl}) = \log\left(\frac{\pi_{itl}}{1 - \pi_{itl}}\right) = \beta_0 + \sum_{m=1}^M \beta_m x_{mi} + r_t + s_l + u_{tl} \quad (4)$$

where  $\beta_0$  is the intercept,  $\beta_m$  ( $m = 1, \dots, M$ ) are fixed effects related to measured covariates ( $x_1, \dots, x_M$ ),  $r_t$  is the temporal effect,  $s_l$  is the location / 'spatial effect' and  $u_{tl}$  is the term of spatiotemporal interaction.

### 3. SPATIOTEMPORAL MODELS USING R-INLA IN BAYESIAN HIERARCHICAL MODELS

#### 3.1 Proposed Solution: BSTHM (Bayesian Spatiotemporal Hierarchical Model)

In the Bayesian Spatiotemporal Hierarchical Model (BSTHM), in terms of space, we denote the  $I$  area units at a zone level by  $I = 1, \dots, I$ . On the temporal plane, we denote the time  $T$  by  $t = 1, \dots, T$ . Let  $y_{it}$  be the values of a variable of interest in zone  $i$  and time  $t$ . All our models assume a prior distribution of log-normal likelihood. The structured additive linear predictor  $\eta_{it} = \log(y_{it})$  will be additively decomposed into space, time, or both components. As mentioned below in the implementation section, we have built three different models. The details are described in this section.

**Parametric spatiotemporal model (Model 1):** This spatiotemporal model is based on the model proposed by Bernardineli and colleagues

$$\eta_{it} = \alpha + \mu_i + v_i + (\beta + \delta_i) \times t \quad (5)$$

In the linear predictor  $\eta_{it}$ ,  $\alpha$  quantifies the fixed effect (intercept), and  $\mu_i$  and  $v_i$  are the spatial components that represent two random effects. The term  $v_i$  supposes a Gaussian a priori exchangeable on the unstructured heterogeneity of the model, formalized in the form  $v_i \sim \mathcal{N}(0, \delta_v^2)$ , and  $\mu_i$  supposes an intrinsic conditional autoregressive a priori (CAR) for the structured heterogeneity spatially.

The spatial components include two effects: one assuming an exchangeable Gaussian a priori that allows to model unstructured heterogeneity, which is  $v_i \sim \mathcal{N}(0, \delta_v^2)$ , and the other assuming an autoregressive a priori intrinsic conditionality (CAR) for spatially structured heterogeneity, which is:

$$\mu_i | \mu_{j \sim i} \sim \mathcal{N}\left(\frac{1}{m_i} \sum_{i \sim j} \mu_j, \frac{\sigma^2}{m_i}\right) \quad (6)$$

Where  $i \sim j$  indicates that the zones  $i$  and  $j$  are neighbors,  $m_i$  is the number of zones sharing the boundaries of the  $i$ th zone and  $\sigma^2$  the variance component. The spatial dependence in  $\mu_i$  assumes the CAR a priori which extends the well-known Besag model and with a Gaussian distribution, which implies that each  $\mu_i$  is conditional on the neighbor  $\mu_j$ , the variance depending on the number of zones neighboring the zone  $i$ . Structured spatial effect is considered as spatial autocorrelation information borrowed from nearby neighbors, and unstructured spatial effects are considered as spatial heterogeneity characteristics in a specific area. Model 1 also includes the linear effect  $\beta$ , which represents the main temporal trend, and a differential temporal trend,  $\delta_i$ , which represents the zone-specific temporal variation (the differential temporal trend for each region).

**Nonparametric spatiotemporal model (model 2):** Knorr-Held and Rasser proposed this model to overcome the limitation suffered by the Bernardineli and colleagues model. As an alternative to the hypothesis of a linear time trend in Model 1, Model 2 implements a general nonparametric dynamic time trend, considered more realistic. It adopts a random walk model for the main temporal trend and the corresponding term of spatiotemporal interaction. The linear predictor of a non-parametric spatiotemporal model can be written as:

$$\eta_{it} = \alpha + \mu_i + v_i + \gamma_t + \phi_t + \delta_{it} \quad (7)$$

Where  $\mu_i$  and  $v_i$  represent the main spatial random effects, identical to those of model 1;  $\gamma_t$  and  $\phi_t$  represent the main temporal effects; and  $\delta_{it}$  represents the space-time interactions. The term  $\phi_t$  represents the unstructured temporal effect and is specified using a normal null-average normal a priori with an unknown variance  $\sigma_\gamma^2$ . The term  $\gamma_t$  represents the structured temporal effect and is modeled dynamically by means of a neighboring structure. We

used the Random Walk (RW) dynamic model as a priori for the structured temporal effect, with its a priori density  $\pi$  is as follows:

$$\pi(\gamma_t | \sigma_\gamma^2) \propto \exp\left(-\frac{1}{2\sigma_\gamma^2} \sum_{t=2}^T (\gamma_t - \gamma_{t-1})^2\right) \quad (8)$$

In the spatiotemporal interaction term  $\delta_{it}$ ,  $i = 1, \dots, I$  is the spatial index and  $t = 1, \dots, T$  is the temporal index. The specification of the a priori on  $\delta_{it}$  depends on the main spatial and temporal effects, which are supposed to interact. Assuming that the main spatial effect  $v_i$  and the temporal main effect  $\gamma_t$  interact, each spatial unit  $\delta_i = (\delta_{i1}, \delta_{i2}, \dots, \delta_{iT})'$ ,  $i = 1, \dots, I$ , follows a random walk, and the a priori on  $\delta_{it}$  is written as follows:

$$p(\delta | k_\delta) \propto \exp\left\{-\frac{k_\delta}{2} \sum_{i=1}^m \sum_{t=2}^T (\delta_{it} - \delta_{i,t-1})^2\right\} \quad (9)$$

Where  $k_\delta$  is the precision factor, which is the inverse of the variance  $\sigma_\delta^2$ . The space-time interactions  $\delta_{it}$  are considered as unobserved covariates for each unit  $(i, t)$  having structures in time and space. Such a specification is appropriate when temporal trends differ from one area to another, but spatial trends are stable. With  $\delta_{it}$ , model 2 can take into account not only the spatial heterogeneity of each zone, but also the temporal variation of each zone over time  $T$  for the imputation of the missing data.

The spatiotemporal interaction effect models the relationship between the temporal and spatial trend. In the model, different types of interaction can be investigated: 1) **Type I**: unstructured space is multiplied unstructured time. Similar temporal pattern across areas and same in magnitude. 2) **Type II**: unstructured space is multiplied structured time (rw1 or ar1, rw2). Similar temporal pattern across areas, but different in magnitude. 3) **Type III**: structured space (Besag) is multiplied unstructured time. Similar spatial pattern across time, but different in magnitude. 4) **Type IV**: structured space (Besag) is multiplied structured time (rw1 or ar1, rw2). No similar patterns across areas or time.

**Multi-variable spatiotemporal regression model (model 3)**: When information about covariates (observed and associated variables) is available to supplement missing values, a traditional multivariable regression model can easily be specified:  $\eta_{it} = \alpha + \sum_k \beta_k X_{itk}$ , where  $\alpha$  quantifies the intercept,  $X_k$  is the  $k$ -th covariate, and  $\beta_k$  are the coefficients. Combining it with Model 2, we build Model 3 as follows:

$$\eta_{it} = \alpha + \sum_k \beta_k X_{itk} + \mu_i + v_i + \gamma_t + \phi_t + \delta_{it} \quad (10)$$

Where the specifications of these spatial and temporal random effects are the same as in Model 2. With this model, imputation can comprehensively incorporate covariates, spatial effects, temporal effects, and space-time interactions.

### 3.2 Implementation of the model

The spatiotemporal modeling process consists of two steps in general. As a first step, we integrated information from spatial data and temporal structures into existing data. We used spatiotemporal models that take into account the random effects of space and time. The second step is to integrate the land cover variables named  $(lc_0, \dots, lc_n)$ , whose missing percentages are important. The second step used multivariable regression modeling because we had the covariates of the first step as independent variables.

In each of the two stages, we constructed two alternative statistical models. In step 1, we constructed two spatiotemporal models, one parametric and one non-parametric (hereinafter referred to as Model 1 and Model 2, respectively). They use the same components of the spatial effects, but the model 1 uses the linear a priori, whereas the model 2 uses the nonlinear a priori for the temporal components and the space-time interaction components. With models 1 and 2, we wanted to know what type of spatiotemporal model best fits our data and we chose the optimal model between the two for the next step. In Step 2, we constructed multivariate spatiotemporal regression models (here called Model 3). Compared to model 2, model 3 includes additional information on covariates (the 3 variables imputed in step 1). Model 3 will demonstrate the utility of the new covariate imputed method in estimating other variables.

After building the models, we used various evaluation and validation methods. First, we evaluated the two pairs of alternative spatiotemporal models (1-on-2 models and 2-on-3 models) for the Bayesian model we used the deviance criterion (DIC) and the predictive quality using the conditional predictive order (CPO). This first step of the evaluation was based on the entire dataset and chose an optimal spatiotemporal model for imputation. Second, we performed cross-validation to evaluate the predictive performance of the spatiotemporal model and the sensitivity of the model to changing a percentage of missing data. Specifically, we randomly sampled 10%, 20%, and 30% of the

existing data to create three test sets, and we used the rest of the data as learning sets. In addition, we obtained the spatial uncertainty intervals to evaluate the local prediction errors of the spatiotemporal models applied in the method. Third, we compared our proposed method with other widely used imputation methods.

We have used the Integrated Nested Laplace Approximation (INLA) implemented in R-INLA within the R statistical software. The R-INLA package solves models using INLA, which is an approach to statistical inference for latent Gaussian Markov random field (GMRF). The approximation is divided in three stages. The first stage approximates the posterior marginal of  $\theta$  using the Laplace approximation. The second stage calculates the Laplace approximation, or the simplified Laplace approximation, of  $\pi(x_i|y, \theta)$ , for selected values of  $\theta$ , in order to improve on the Gaussian approximation. The third process combines the previous two using numerical integration.

#### 4. APPLICATION ON SPATIOTEMPORAL MODELING OF FIRE OCCURRENCE

##### 4.1 Study area and dataset

The study area is in the Ankarafantsika National Park (ANP) which is located in the northwestern part of Madagascar, the latitude varies between 16 ° 09 'and 16 ° 26' South then the longitude varies between 46 ° 13 'and 46 ° 33' East. It is part of one of the largest protected areas (with the two other integral nature reserves) of the Boeny region and with an area of 130,026 ha. Administratively, it is constituted by twenty-six (26) administrative units or "fokontany".

The dataset we used is the remote sensing dataset from MODIS (Moderate Resolution Imaging Spectroradiometer), which is mounted on two NASA satellites and identifies fires based on changes in reflectance and temperature at ground level. The fire data analyzed are the MODIS AFP satellite products (Active Fire Products, MCD14DL archives distributed by the University of Maryland), which provide the geographic coordinates of all fires detected over the period 2000-2018 at the daily scale.

##### 4.2 Temporal models

The results in the previous section suggest that Cox processes are a possible model for describing the occurrence of forest fires. They are frequently applied to aggregated spatial point models, where aggregation is due to stochastic environmental heterogeneity. In this sense, it is possible to use the Bayesian framework to model these procedures.

**Table -1** shows the DIC and WAIC values for the conventional approach to modeling the total number of fires as a function of time. From the values of DIC and WAIC, it is possible to understand that the appearance of fires is structured (linked) over time.

**Table -1:** DIC and WAIC values for different time models

|                         | Model | DIC     | WAIC    |
|-------------------------|-------|---------|---------|
| <b>Linear trend</b>     | -     | 6949.21 | 7148.66 |
| <b>Non-linear trend</b> | iid   | 5561.65 | 5972.11 |
|                         | rw2   | 5562.18 | 5974.14 |
|                         | rw1   | 5561.88 | 5973.32 |
|                         | crw2  | 5562.58 | 5974.80 |
|                         | mec   | 5561.57 | 5971.27 |
|                         | meb   | 5561.64 | 5972.05 |

##### 4.3 Spatial models

Models with the spatial component were then calculated. The summary of results is given in **Table -2**. The first spatial model is a classical random effects model; it has been calculated in order to access the susceptibility level of

each zone and to have a reference base to compare with other models. The DIC on the model is 3196.29 and WAIC is 3455.81. The log score is 4.099, the Brier Score is 285.50, and the CVM test (on PIT values) 8.42, the p-value is 7.347e-11. The Brier score is indicative of a bad model. The CVM also indicates a bad model, once the p-value should be greater than 0.10 at least, to indicate a uniform distribution. The fixed effect, intercept, has an average of -1.5285 with a standard deviation of 0.3769 (95% CrI -0.919, -2.156). These values are translated into mean values of 0.2168662, with a standard deviation of 1.457822 (95% CrI 0.3989209, 0.1157818), when they are exponential. This, in turn, would indicate that fires throughout the park increased by 28% during the period considered at a rate of 0.55% per year.

The density of the random effects distribution for this model, a term of interest, is given in **Chart -1** and shows that they are not really normally distributed and, even when approximating, they are not symmetric around zero, which could prove that this model is not a good approximation of reality. **Fig -1** shows us the map of these effects, for the same model. They indicate the overall risk for each administrative unit.

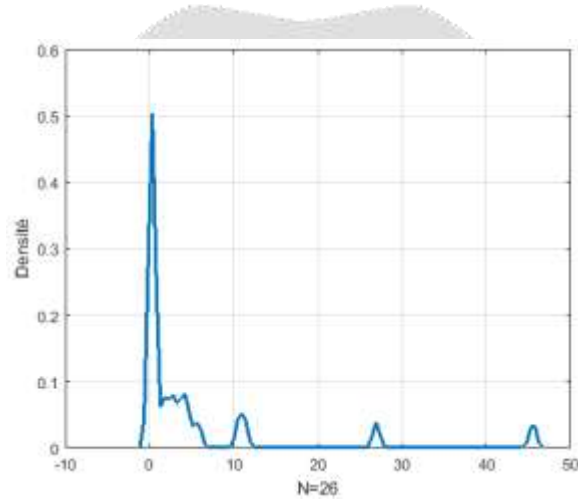


**Chart -1:** Density of the random effects distribution

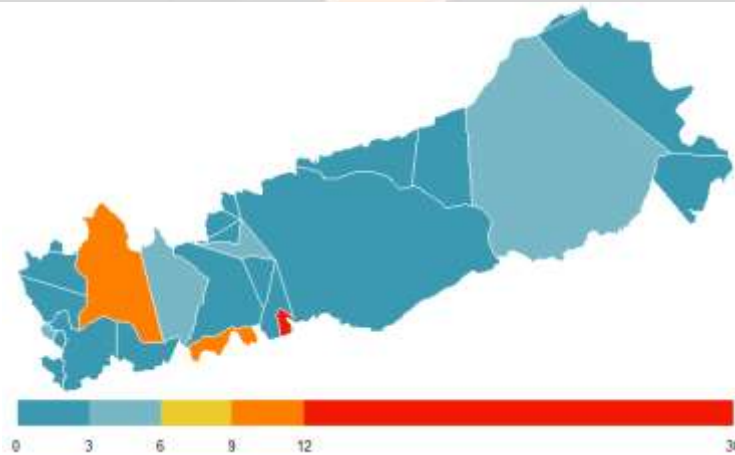


**Fig -1:** Map of unstructured random effects

The administrative unit or fokontany most exposed to fire is Ambodimanga (marked in red), followed by Betaramahamay and Belalitra (marked in orange).

**Table - 2:** Summary of the results between the different spatial models

| Models            | DIC     | WAIC    | Log score | Brier score | CVM                  | Fixed effects |        |           |        |
|-------------------|---------|---------|-----------|-------------|----------------------|---------------|--------|-----------|--------|
|                   |         |         |           |             |                      | Intercept     | SD     | Quantiles |        |
| Classic model     | 3196.29 | 3455.81 | 4.099365  | 285.5089    | 7.34e <sup>-11</sup> | 0.2168        | 1.4578 | 0.3989    | 0.1157 |
| Convolution model | 3196.31 | 3455.80 | 4.099357  | 285.5083    | 7.36e <sup>-11</sup> | 0.2166        | 1.4602 | 0.3993    | 0.1154 |

**Convolution model:**

The next model to calculate was the convolution model. This model adds a structured spatial component to the first spatial model. Results for this model include a DIC of 3196.31, a WAIC of 3455.80 and a Brier Score which decreased slightly (285.5083). The decrease in these values (except DIC), compared to the first model, may indicate that the insertion of the spatial structure into the NAP fire modeling technique has a positive effect on the quality of the model. Nevertheless, the values of the log score (4.099357) and the p-value of CVM always reflect poor predictive quality. **Chart -2** and **Chart -3** show respectively the density curves for the distribution of unstructured effects and the spatial distribution of the structured effects.

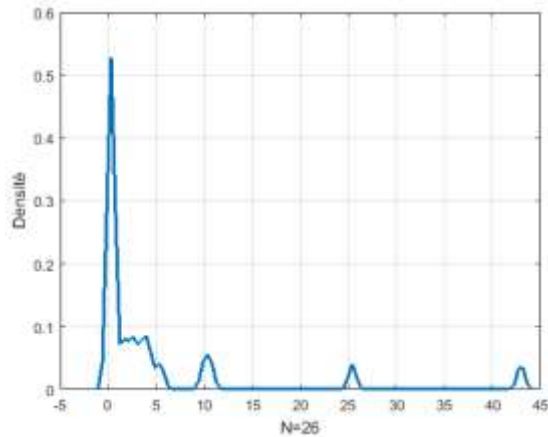


**Chart -2:** Density: distribution of unstructured effects

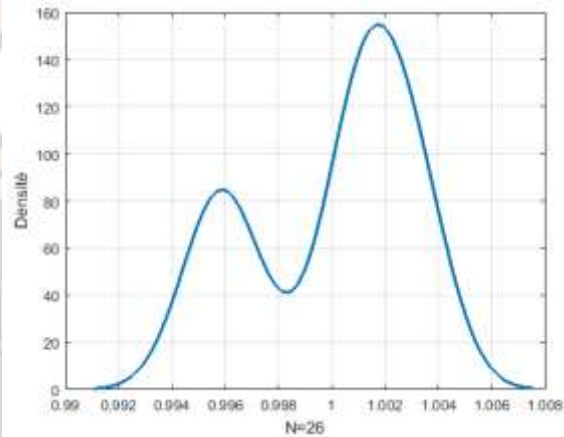


**Chart -3:** Density: spatial distribution of structured effects

Both must be symmetrical around zero and normally distributed, which happens to a certain extent. Both distributions are roughly centered around a threshold. This indicates that there is another heterogeneity in the model that needs to be taken into account. **Fig -2** and **Fig -3** show the maps for the random effects and spatial effects of this model, respectively.

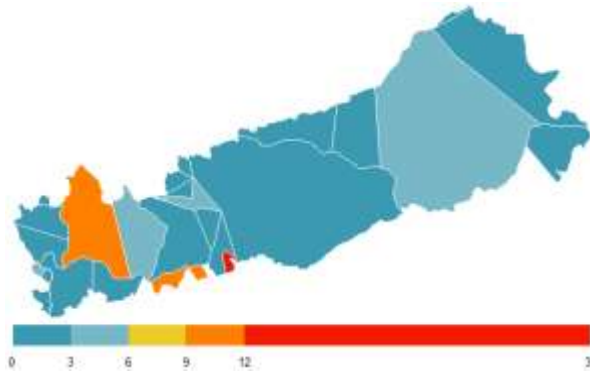


**Fig -2:** Map of unstructured random effects

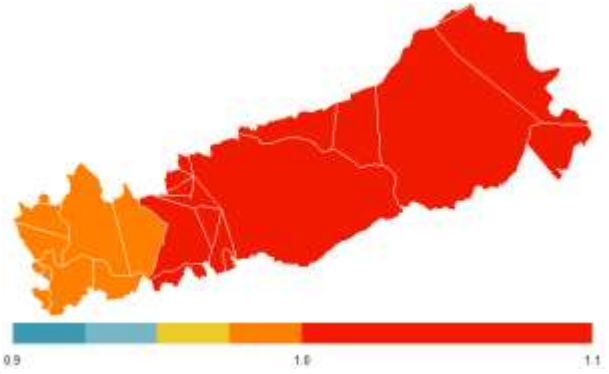


**Fig -3:** Map of structured spatial effects

They are presented to gain a better understanding of the modeling technique that affects how the occurrence of fires is given for each administrative unit. In Figure 5.13, there are no spatial data effects. Structure how the fires are modeled, but on the other hand, the neighboring spatial structure is taken into account in **Fig -3**, where the risk is different. In fact, the spatial structure seems to mitigate the facts, even if the most inclined administrative units are still highlighted. These are shown separately, but they can be merged into a single prediction model that reflects the global fire occurrence, shown in **Fig -4**. The map of this value corresponds to  $\theta$ , given by  $\beta_0 + u_i + v_i$  and represents the global data that are now adapted by the model. A spatial risk map  $\zeta$  given by  $\zeta = u_i + v_i$  can also be calculated from the margins values of the model (**Fig -5**) and displays the administrative units that have a higher probability of fire risk, as part of this model.

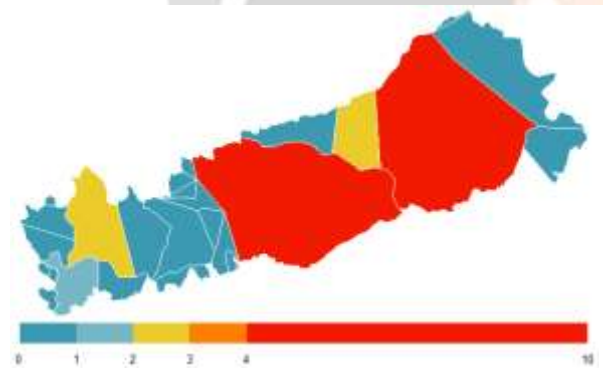


**Fig -4:** Overall Occurrence of fires

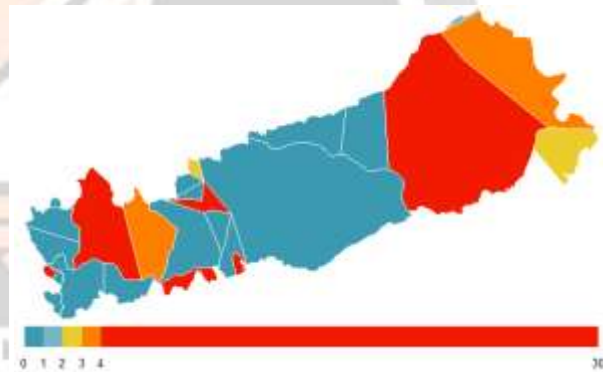


**Fig -5:** Fire risk, spatial convolution model

With the convolutional space model, Considering the effects taken into account, we can now observe that the most fire-exposed administrative units are Ambodimanga, followed by Betaramahamay, Belalitra, Andranomangatsiaka, Ambikakely, and Belinta.



#### 4.4 Spatiotemporal models

##### BYM model with an unstructured temporal component

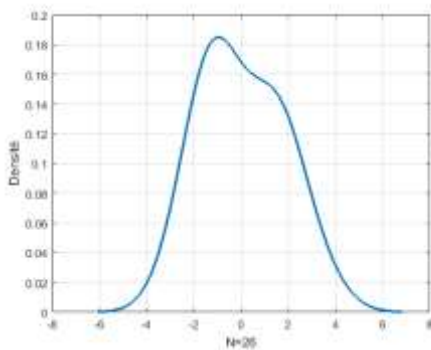


**Chart -4:** Unstructured spatial component

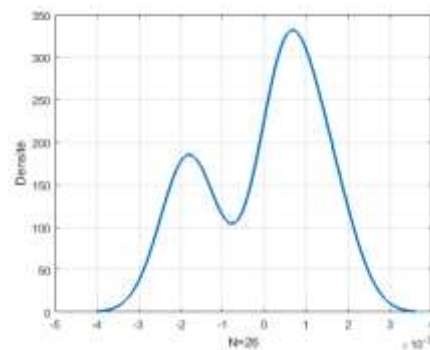


**Chart -5:** Structured spatial component

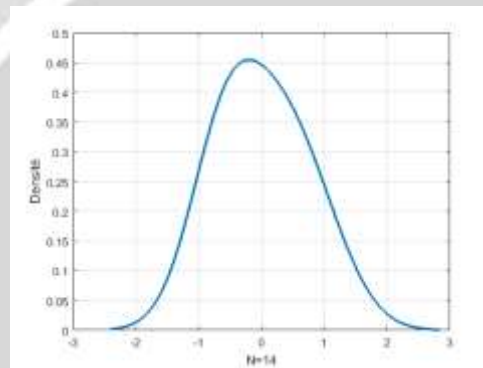


**Chart -6:** Density for the distribution of unstructured temporal effects

An unstructured temporal component has been assigned to the BYM formulation and the following model has been calculated. The DIC for this model is 992.25 and the WAIC is 963.77, with a log score of 3.8229. The values of DIC and WAIC are much lower than those of the latest models without time component, the log score indicates a better fit of the model. The Brier score is 4.59 and the p-value of the CVM is 0.0004619. These latter values suggest that the quality of the predictive model is better than that of the model without the temporal component; this time, the Brier score was much smaller, and the PIT seemed to tend towards a uniform distribution. The intercept is now 0.4981 (CrI at 0.2175, 1.1042 at 97.5%).

**Chart -4, Chart -5 and Chart -6** show the density curves for spatial random effects distribution, spatial structured effects, and unstructured temporal effects for this model.

All distributions now show a major concentration around zero. It is a sign of improvement of the model. Even if they are not symmetrical: they present a bump on the right or left side it still reflects a certain geographical and temporal geographical heterogeneity that is not taken into account.

## BYM model plus a structured temporal component and with hyperparameters for weak prior information

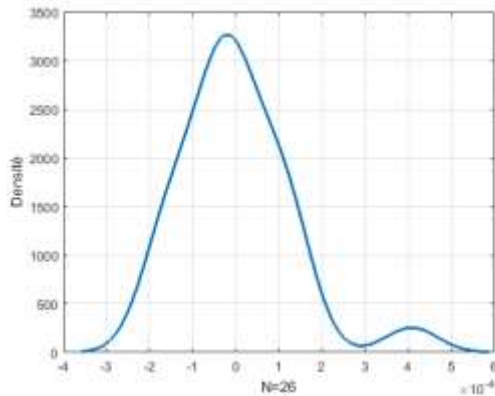


**Chart -7:** Unstructured spatial component

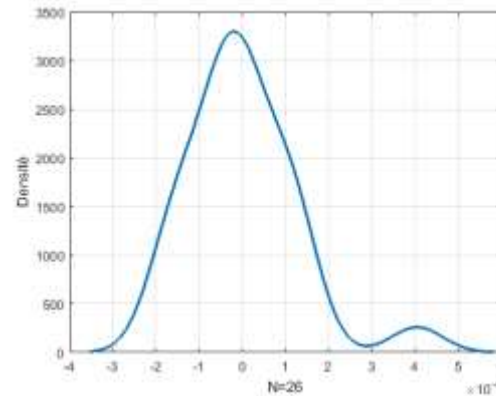


**Chart -8:** Structured spatial component

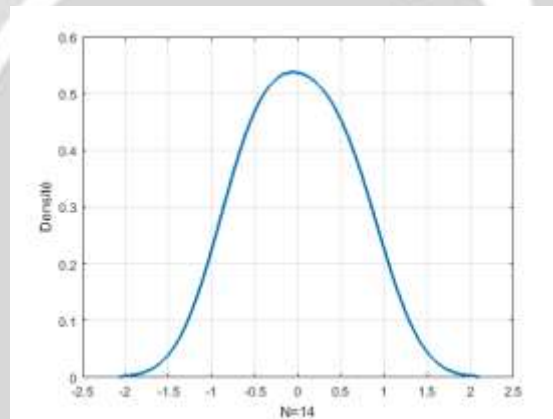


**Chart -9:** Structured temporal component

The modification made to this model concerns the distribution a priori not very informative. With R-INLA, we can specify using the option `hyper` (hyperparameters) in the specification of the formula these a priori uninformative. Note that we now use the informative a priori on the Log of the precision of the structured effect (35, 0.001) and the precision of the unstructured effect (35, 0.00001). The improvement of its spatial fraction is simply to define a larger precision (or a smaller equivalent variance) for the spatially rather than unstructured structured effect. In defining this new distribution a priori for the structured and unstructured effect, the spatial fraction increased about 81.72%. We will therefore use this hypothesis for the BYM specification in the hierarchical Bayesian model.

The DIC and WAIC are now 1121.68 and 1102.87, with a log score of 8.0129. The value of the criterion DIC and the value of the criterion WAIC are superior compared to the last model (even the Brier score 4.7888). On the other hand, the p-value is slightly improved. The intercept is now given by an average of 0.5245 (97.5% CRI 0.7009, 0.0.3838). **Chart -7, Chart -8 and Chart -9** show the random effects for the different spatiotemporal components of the model.

As for the last model, there is a component in the spatial variability that the model can not explain, given by the bimodal appearance of the spatial random effect and the structured spatial component. Nevertheless, it seems that this explains the temporal variability, given the almost perfect symmetry of temporal random effects.

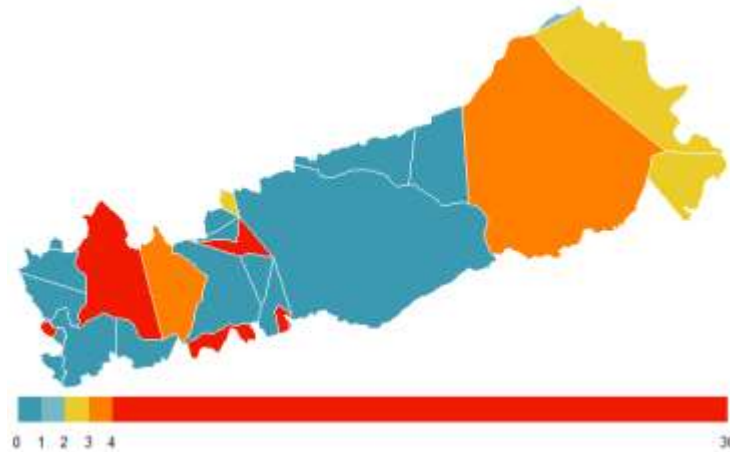


**Fig -6:** Space effects averaged over all years from 2005 to 2018

**Fig -6** shows the average adjusted spatial effects for this model for all years from 2005 to 2018. The insertion of the structured temporal component dissolved some of the adjusted values. Some events in administrative units where there more fire is decreased in the adjusted value class. This is because some trends can now be explained by the time trend.

The marginal terms presented in **Fig -7** used this same principle. The maximum probability of fire in an administrative unit was 2 years, in a year to come. But with the insertion of the temporal component, this maximum value has been reduced to 1, which is again justified by the fact that the distribution affects the process of modeling the appearance of fires.

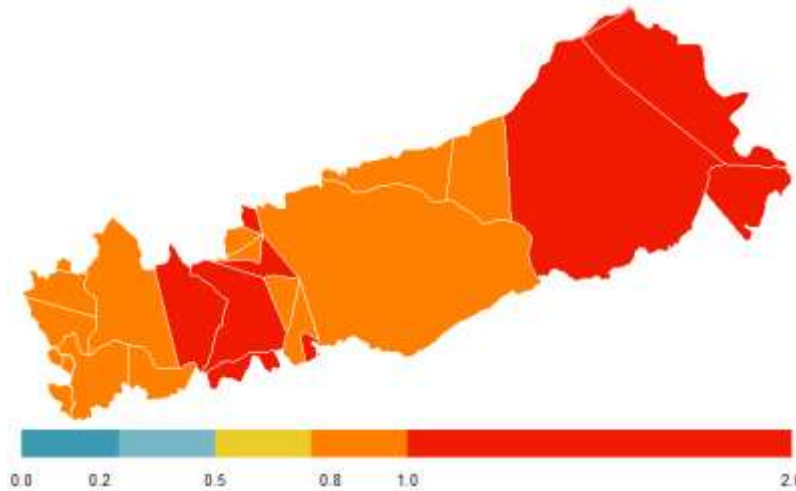


**Fig -7:** Random effects: spatiotemporal risk of fire occurrence in ANP

These results can also be seen in another way. **Fig -8** shows the fire occurrence rate map in Ankarafantsika National Park and its random error. Areas (administrative units) with higher fire occurrence concentrations are those that represent more variability. This is because the more samples there are in a given state, the variability will necessarily increase.

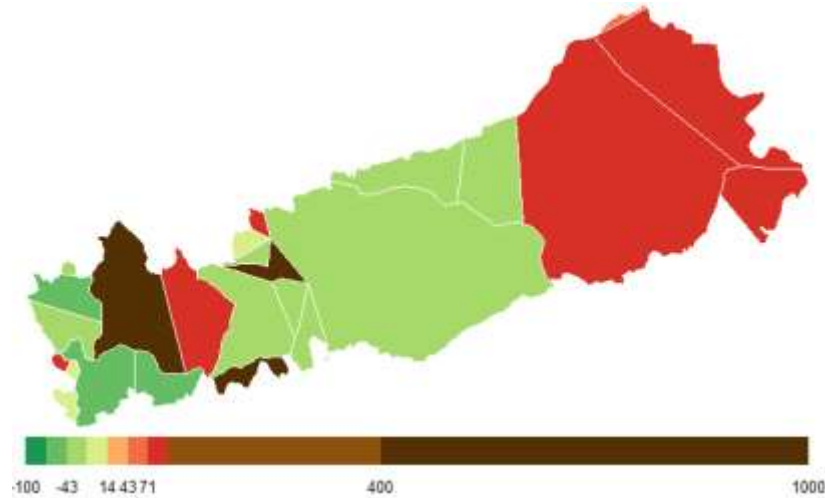


**Fig -8:** ANP fire occurrence map

The standard error map is shown in **Fig -9**. We noticed that some errors are still significant (between 1 and 4). This model is not yet a good approximation of reality.

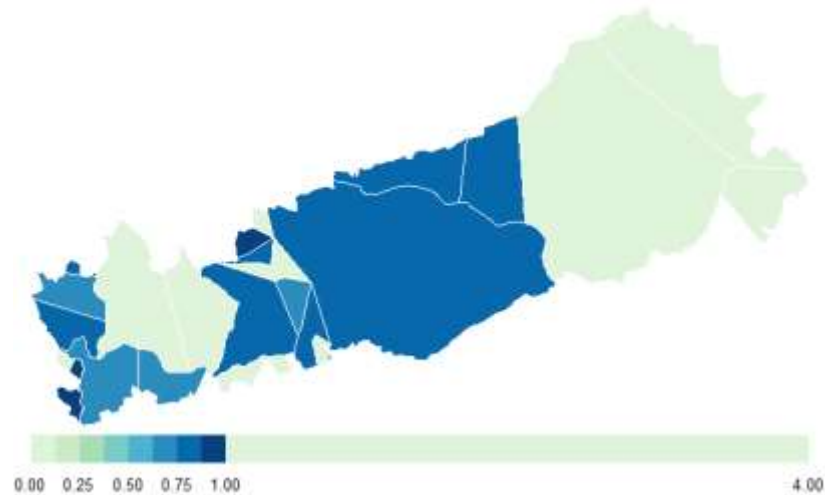


**Fig -9:** Map of standard errors

### Multi-variable spatiotemporal regression model

Covariates explain much of the variability of a spatiotemporal model and, in this sense, they were added at this stage of the modeling process, before analyzing the temporal component and adding more noise into the model. In this sense, other indications of the quality of the model with the inclusion of covariates should be taken into account. Thus, a model with a spatial BYM formulation, plus a structured temporal component, plus covariates, was calculated, and the distribution of the later marginals were accessed.

After some analysis on the correlation of each covariate with respect to the occurrence of fires. It can be seen that the only factor that does not affect, or does not relate to, the occurrence of fires is the water points. Climatic data such as precipitation and temperature have a major contribution to the occurrence of fire. The rest of the land cover classes also appear to have an influence on fire distribution.

The mean values of the fixed effects indicate that the fire frequency varies in proportion to the increase in all covariates, those that seem to facilitate the occurrence of fires and, except for the water points, which do not appear to have relationship with fire distribution (this would only influence the fire) by 0.01%. In this sense, the water point will be the only covariate that will not be taken into account in future formulations of the model. Now that covariates are selected, it is time to explore the spatiotemporal trends in the occurrence of ANP fires.

**Chart -10, Chart -11 and Chart -12** show the random effects for the different spatiotemporal components of the model. These three curves are approximately symmetrical around zero and the three densities are closer to a Gaussian distribution than the other models.

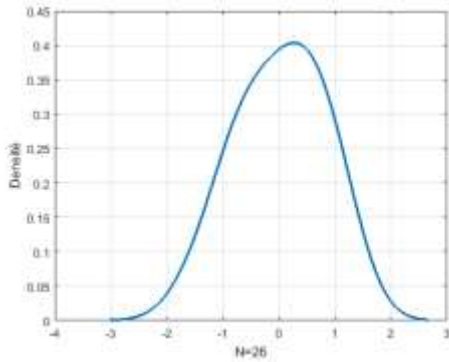


**Chart -10:** Unstructured spatial component

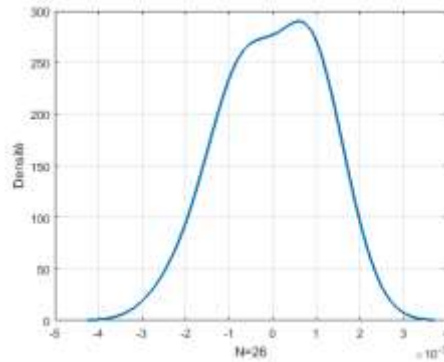


**Chart -11:** Structured spatial component

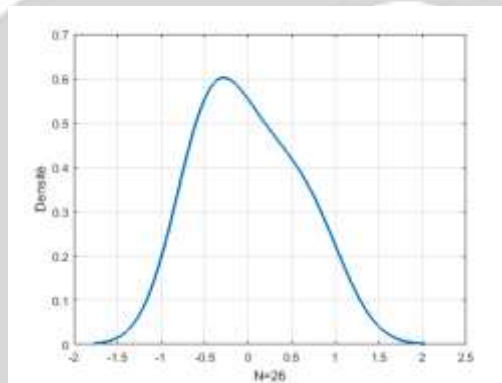


**Chart -12:** Structured temporal component

$$y_i \sim \text{Poisson}(\lambda_i \theta_i)$$

$$y_{it} = \beta_0 + u_i + v_i + \gamma_t + \phi_t + \delta_{it} + \sum \beta_n x_n$$

Where  $\beta_0$  is the intercept,  $u_i$  is the unstructured random effects spatial component with a normal distribution and a zero mean, and  $v_i$  is a spatial component with a conditional autoregressive structure; the term  $\gamma_t$  represents the structured effect over time, dynamically modeled.  $\phi_t$  is specified by means of a Gaussian exchangeable prerequisite:  $\phi_t \sim \text{Normal}(0, 1/\tau_\phi)$ , and  $\delta_{it}$  represents the interaction between space and time, which is unstructured, and  $\sum \beta_n x_n$  are climatic effects and the percentage of different types of land use.

These values indicate that all covariates have a positive influence on fire occurrence, with the exception of different forest types, and for each percentage increase in land cover, the risk of fire occurrence increases by 1 % for this state. In addition, all types of land cover that increase the occurrence of fires allow the influx of low levels to flow. The forest acts as an accelerator for the tangential speed of fires. In this case, the results make sense.

**Fig -10** shows the spatiotemporal effects adjusted in averages, given by  $\theta$ .

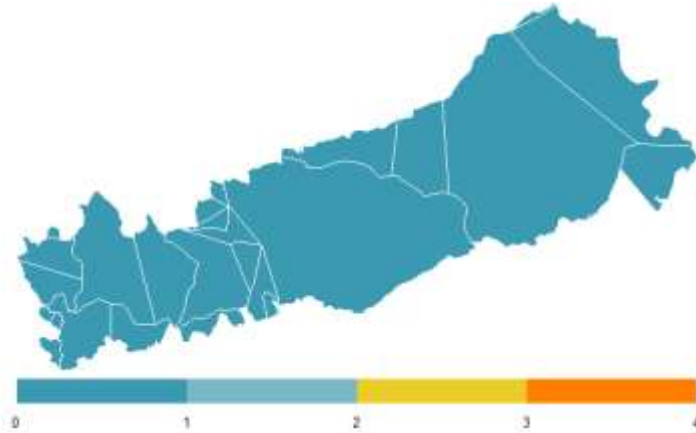


**Fig -10:** Spatiotemporal effects adjusted to mean

It is the spatiotemporal averages of the fires that the model can explain for each administrative unit. In addition, **Fig -11** also gives a spatial risk map. This is now interpreted as the residual relative risk for each zone (compared to the entire park).

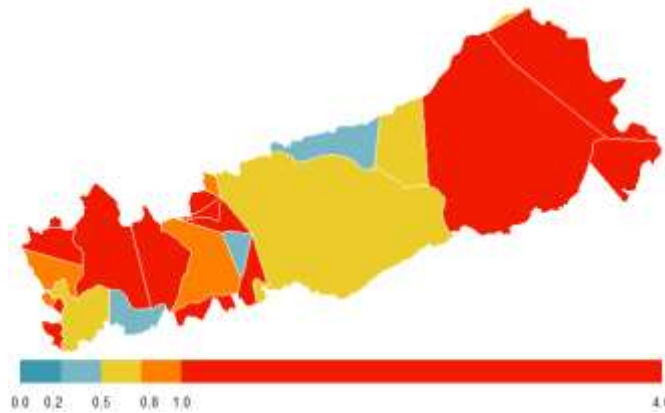


**Fig -11:** Residual relative risk map for each zone

In interpreting this figure, the maximum fire probability in an administrative unit was 4 years, in a year to come. But with the insertion of the temporal component, this maximum value has been reduced to 1, which is justified once again by the fact that the distribution affects the process of modeling the appearance of fires.

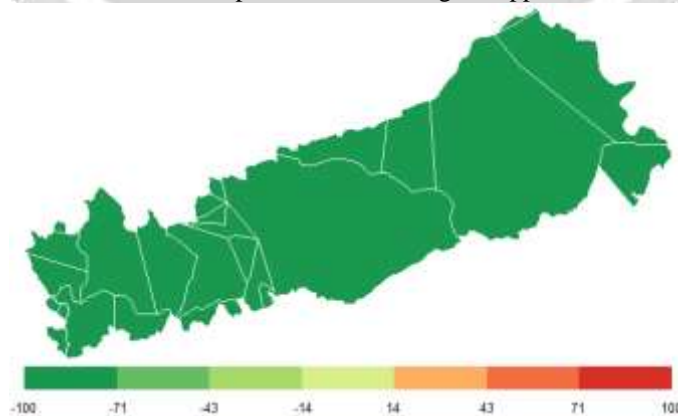


**Fig -12:** Map of ANP fire occurrence rate

These results can also be seen in another way. **Fig -12** shows the map of fire occurrence rate at the ANP and its random error. And the standard error map **Fig -13** for this model is as follows:

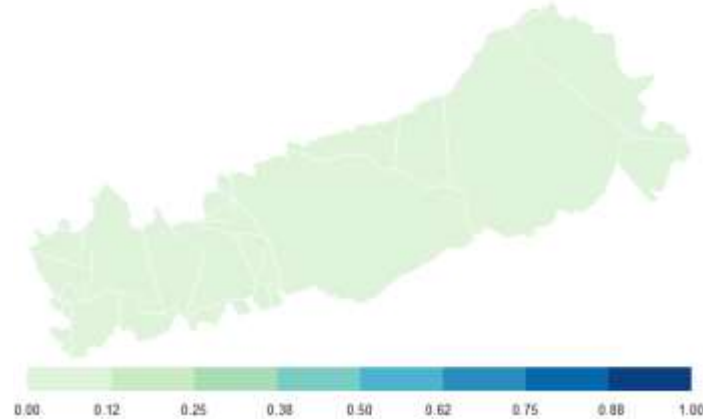


**Fig -13:** Map of standard errors

We noticed that the standard error for the 26 administrative units is less than 0.12, an error that shows a good result for this model.

#### 4.5 Discussion

This article explores the application of spatiotemporal models used in modeling the spatiotemporal distribution of multiple structures phenomena (such as the occurrence of fires). These models have been adapted to forest fire occurrence data in ANP. Integrated Nested Laplace Approximations (INLA) was used for the simulation of posterior distribution parameters. The DIC, WAIC, CPO ... for each model were compared and the best model was selected from the set of candidate models used to fit the fire occurrence data in ANP. Among the spatiotemporal models considered, the model proposed by Knorr-Held and Rasser with a type III and IV space-time interaction corresponds well to the data, but type IV seems better than type III. The variation in the risk of fire occurrence is observed among the 26 administrative units of the ANP and is grouped among administrative units with a high relative risk of fire occurrence. We found concentration and heterogeneity of risk among high-rate regions, and the overall risk of fire occurrence increased slightly from 2002-2009. It has been found that the interaction of the relative risk of fire occurrence in space and time increases in the administrative units many more villages that share borders with the urban administrative units at high risk of occurrence of fire. This is due to the ability of the models to borrow from neighboring administrative units, so that nearby administrative units have a similar risk.

## 5. CONCLUSION

We recommend the Knorr-Held and Rasser model with a type IV space-time interaction structure for modeling and mapping the relative risk of fire occurrence. Risk groupings and high risks are generally observed in the administrative units located in the peripheries of the park (near villages). We have discovered an interesting association between time trends of interaction parameters and migration in ANP, which could provide a framework for further research. Modeling of risk in space and time is quite a challenging task. Although these approaches are less than ideal, we hope that our formulations provide a useful stepping stone into the development of spatiotemporal methodology for modeling and mapping of forest fire occurrence data in ANP.

We are satisfied that the models selected in this paper are from an appropriate class that led to the analysis of fire occurrence data for the period 2005-2018. Further research is required for a standard or acceptable distribution type for space-time interaction  $\delta_{it}$  to be identified since comparing posterior deviance from interaction type that assumed  $\phi_t$  should be modeled as structured could lead to one or more deficiencies to a given interaction type.

**REFERENCES**

- [1] F. Bonneu. Exploring and modeling fire department emergencies with a spatiotemporal marked point process, *Case Studies in Business Industry and Government Statistics*, 139-152, 2007
- [2] Gabriel E. et Diggle P.J. Second-order analysis of inhomogeneous spatiotemporal point process data, *Statistica Neerlandica* , 63, 43-51, 2009.
- [3] H. Rue H, Approximate Bayesian inference for latent Gaussian models by using integrated nested Laplace approximations, *J R Stat Soc Ser B* 71, 2009
- [4] N. Pelekis, B. Theodoulidis, and Y. Theodoridis, Literature review of spatio-temporal database models, *The Knowledge Engineering Review*, 19(03) :235–274, 2004
- [5] R. H. Güting, An introduction to spatial database systems, *The International Journal on Very Large Data Bases*, 3(4) :357–399, 1994
- [6] G. Langran, *Time in geographic information systems*, CRC Press, 1992
- [7] J. F. Roddick and M. Spiliopoulou, A bibliography of temporal, spatial and spatiotemporal data mining research, *ACM SIGKDD Explorations Newsletter*, 1(1) :34–38, 1999
- [8] N. Cressie and C. K. Wikle, *Statistics for spatio-temporal data*, John Wiley & Sons, 2011
- [9] J. Besag, Bayesian image restoration with two applications in spatial statistics, *Ann Inst Stat Math* 43(1), 1991
- [10] L. Serra, Spatio-temporal log-gaussian cox processes for modelling wildfire occurrence: the case of catalonia, *Environmental and Ecological Statistics*, 2014

